

Two Polymolybdate-Based Complexes and Their Graphene Composites with Visible-Light Photo-Responses

Hai-Qiang Luo,^a Pan Zhang,^a Yong-Xi Yang,^a Yun Gong^{*a} and Jian-Hua Lin^{*a, b}

^a Department of Applied Chemistry, College of Chemistry and Chemical Engineering,
Chongqing University, Chongqing 400030, P. R. China. Tel: +86-023-65106150 E-mail:
gongyun7211@cqu.edu.cn

^b State Key Laboratory of Rare Earth Materials Chemistry and Applications, College of
Chemistry and Molecular Engineering, Peking University, Beijing 100871, P. R. China Tel: +86-
010-62753541 E-mail: jhlin@pku.edu.cn

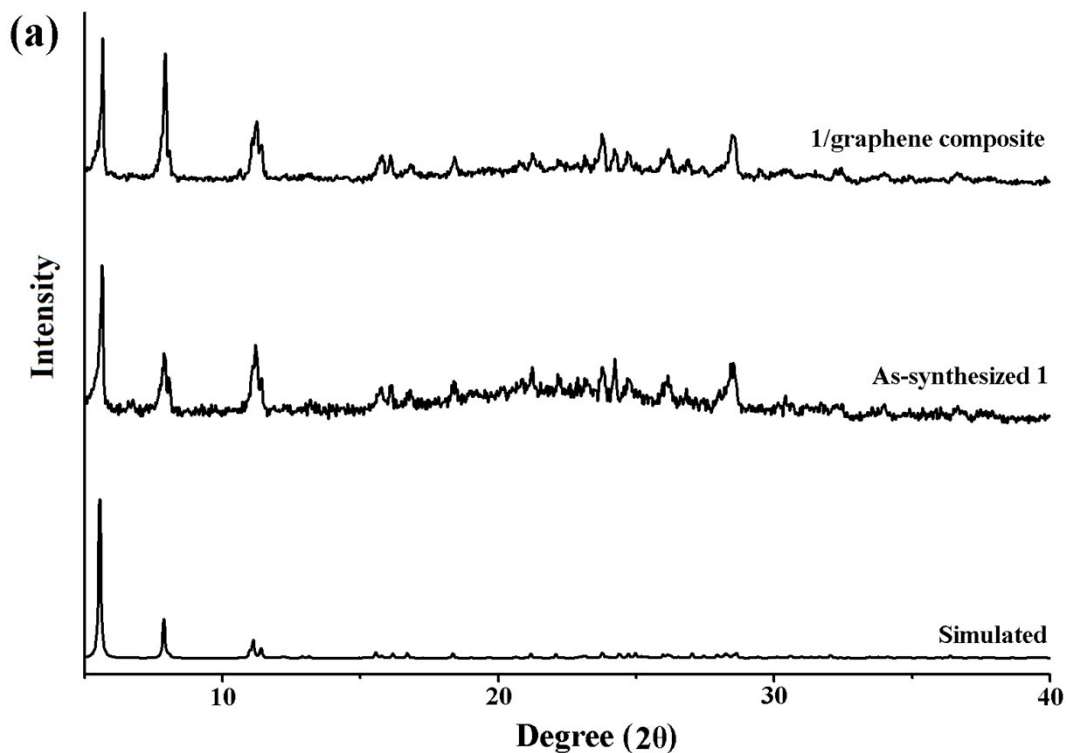
Table S1 Selected bond lengths (Å) and angles (°) for complexes **1** and **2**

<i>Complex 1</i>			
Mo(1)-O(6)	1.67(17)	Mo(1)-O(1)	2.34(14)
Mo(2)-O(10)	1.69(15)	Mo(2)-O(1)	2.35(14)
Mo(3)-O(12)	1.70(13)	Mo(3)-O(11)	2.33(14)
Mo(4)-O(13)	1.78(19)	Mo(4)-O(2)	2.47(15)
O(2)-Mo(1)-O(1)	73(5)	O(5)-Mo(1)-O(1)	165(6)
O(7)-Mo(2)-O(1)	68(6)	O(8)-Mo(2)-O(3)	160(4)
O(4)-Mo(3)-O(2)	71(8)	O(8)#1-Mo(3)-O(11)	173(5)
O(2)#2-Mo(4)-O(7)	73(8)	O(13)-Mo(4)-O(2)	178(6)
<i>Complex 2</i>			
Mo(1)-O(5)	1.693(3)	Mo(1)-O(1)	2.209(3)
Mo(1)-N(2)	2.428(4)	Mo(2)-O(8)	1.699(3)
Mo(2)-O(1)	2.203(3)	Mo(2)-N(8)	2.456(4)

Mo(3)-O(9)	1.698(3)	Mo(3)-O(6)	2.224(3)
Mo(4)-O(11)	1.703(4)	Mo(4)-O(13)	1.9230(16)
Mo(4)-N(3)	2.322(4)	Mo(4)-N(4)#3	2.443(4)
O(2)-Mo(1)-O(1)	72.90(12)	O(5)-Mo(1)-O(1)	162.19(15)
O(3)-Mo(1)-N(2)	78.32(14)	O(4)-Mo(1)-N(2)	176.00(15)
O(6)-Mo(2)-O(1)	72.97(11)	O(8)-Mo(2)-O(1)	156.47(14)
O(6)-Mo(2)-N(8)	74.00(12)	O(7)-Mo(2)-N(8)	170.99(15)
O(6)#4-Mo(3)-O(6)	71.84(13)	O(9)-Mo(3)-O(6)	155.72(15)
O(11)-Mo(4)-O(13)	99.08(14)	O(3)-Mo(4)-O(13)	145.40(16)
O(13)-Mo(4)-N(4)#3	76.13(13)	O(11)-Mo(4)-N(4)#3	167.12(16)
O(11)-Mo(4)-N(3)	90.48(17)	N(3)-Mo(4)-N(4)#3	76.77(13)

Symmetry transformations used to generate equivalent atoms:

#1 $x-1,y,z$ #2 $-x+1,-y+1,-z+1$ #3 $-x+1,y,-z+1/2$ #4 $-x+3/2,-y+3/2,-z+1$



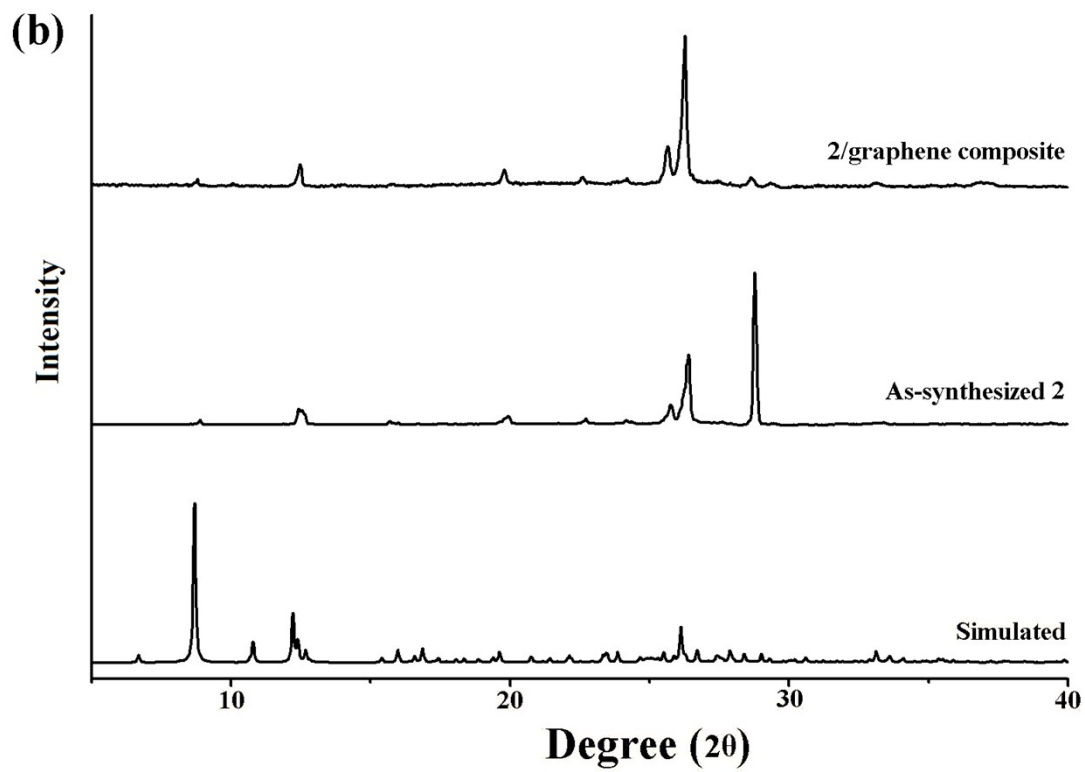
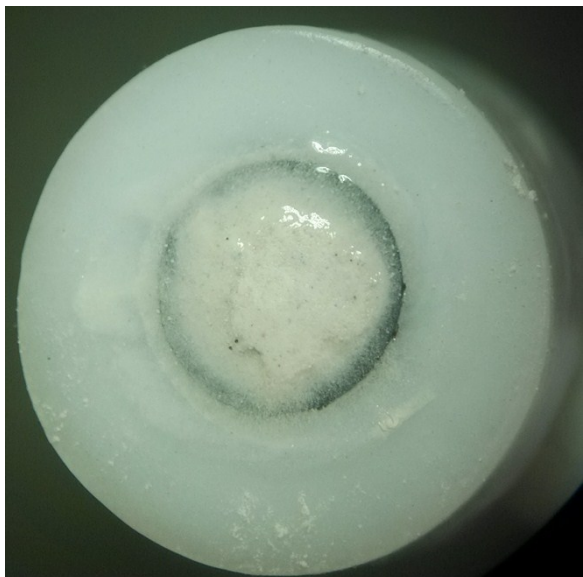


Fig. S1 The PXRD patterns of complexes **1**, **1/graphene composite** (a), **2** and **2/graphene composite** (b).

(a)



(b)



(c)



(d)



Fig. S2 The optic micrograms (40-fold magnified) of **1-GCE** (a), **1/graphene-GCE** (b), **2-GCE** (c) and **2/graphene-GCE** (d).

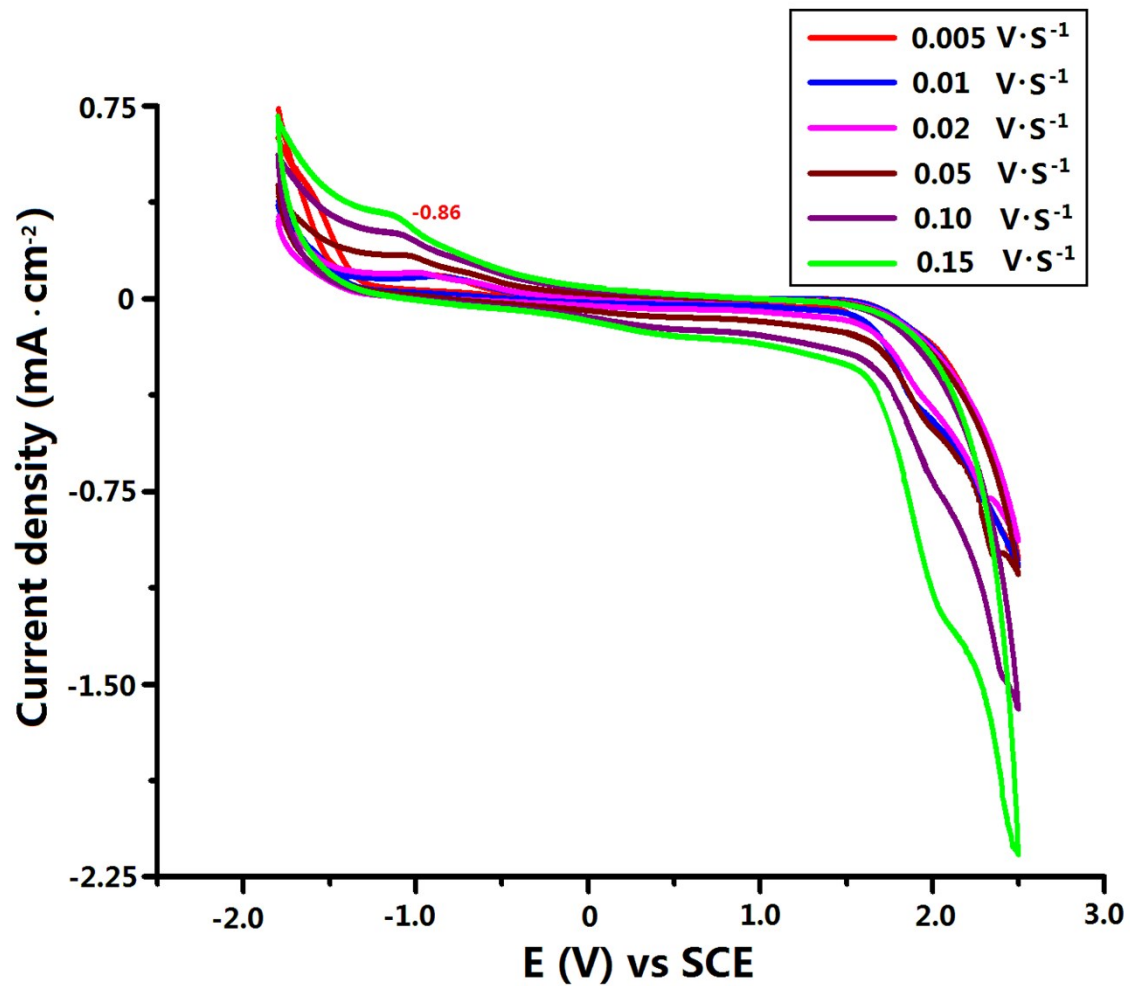


Fig. S3 CVs of the bare GCE in a 0.4 M acetic acid- sodium acetate buffer solution (pH = 4.5, 50 mL) in the potential range from -1.8 to 2.5 V vs SCE at different sweep rates.

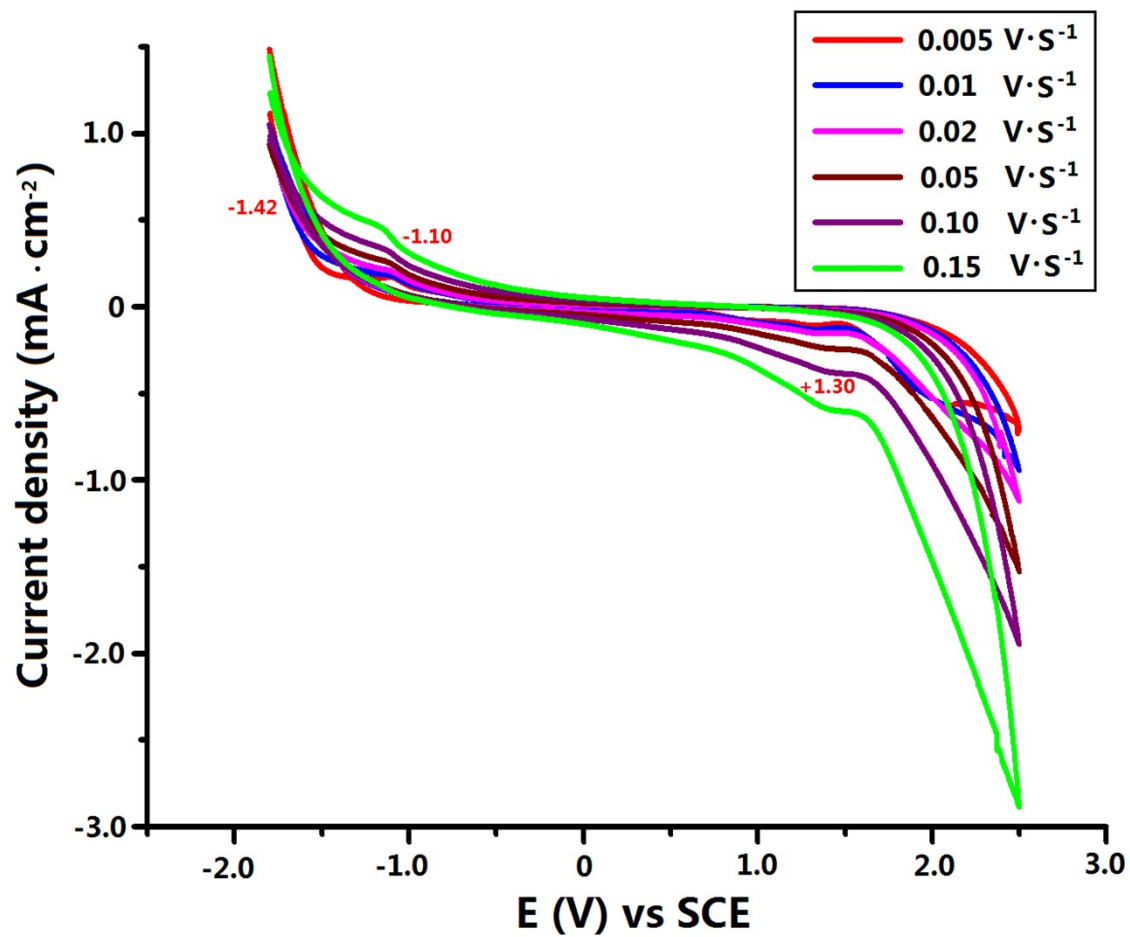


Fig. S4 CVs of L1-GCE in a 0.4 M acetic acid- sodium acetate buffer solution (pH = 4.5, 50 mL) in the potential range from -1.8 to 2.5 V vs SCE at different sweep rates.

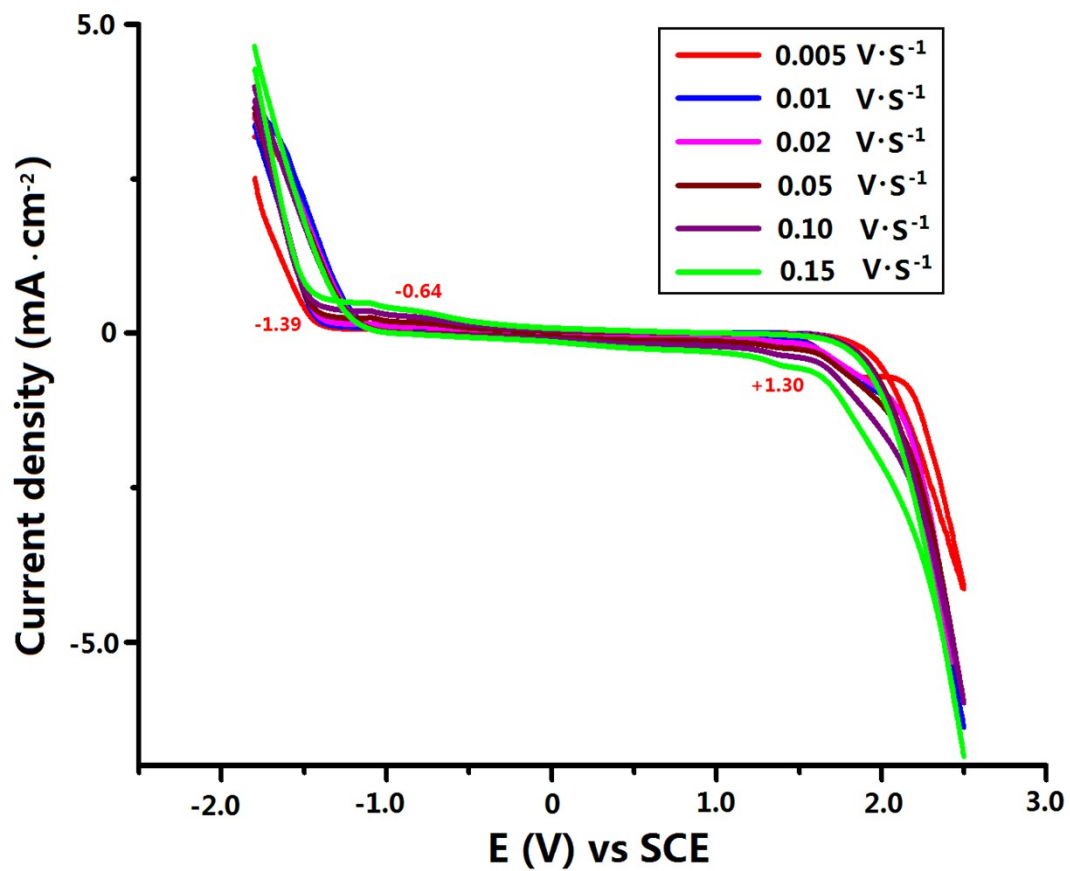


Fig. S5 CVs of 1-GCE in a 0.4 M acetic acid- sodium acetate buffer solution (pH = 4.5, 50 mL) in the potential range from -1.8 to 2.5 V vs SCE at different sweep rates.

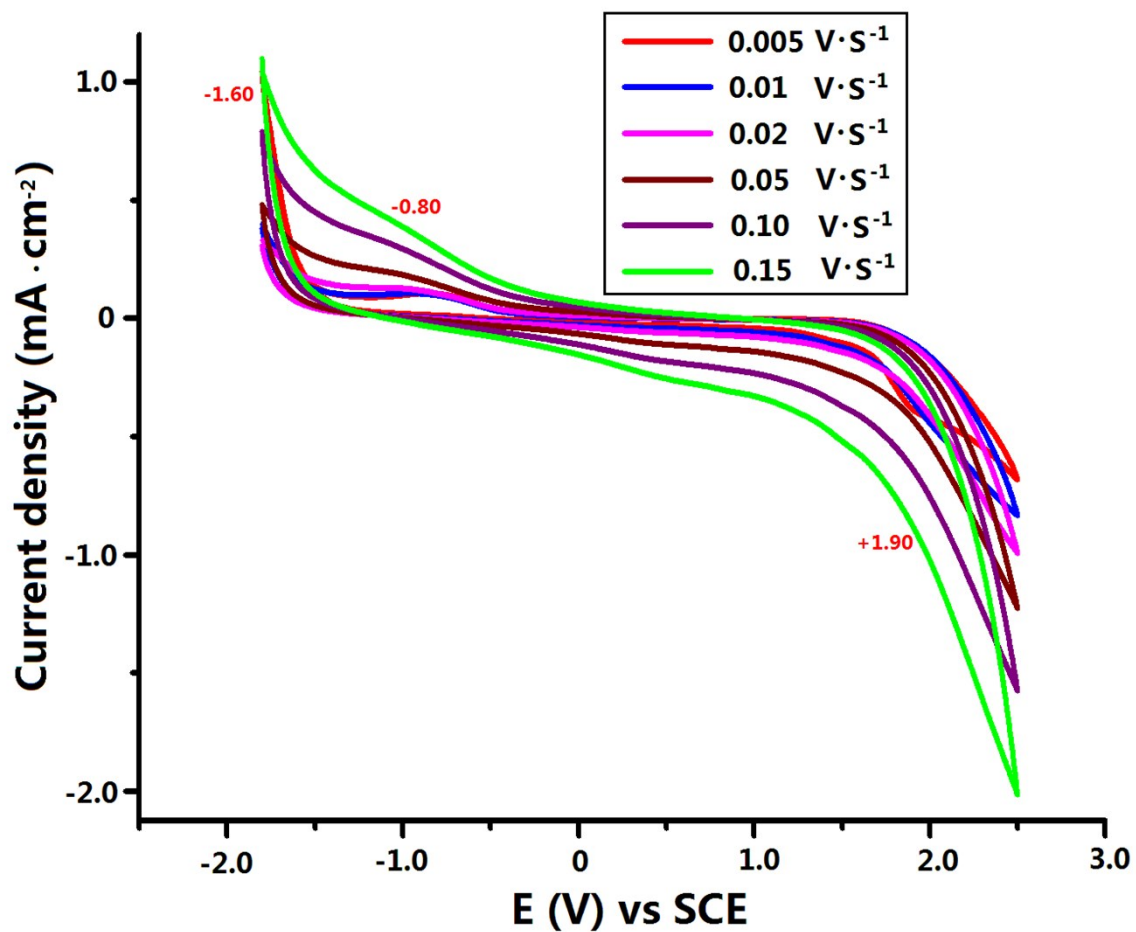


Fig. S6 CVs of L2-GCE in a 0.4 M acetic acid- sodium acetate buffer solution (pH = 4.5, 50 mL) in the potential range from -1.8 to 2.5 V vs SCE at different sweep rates.

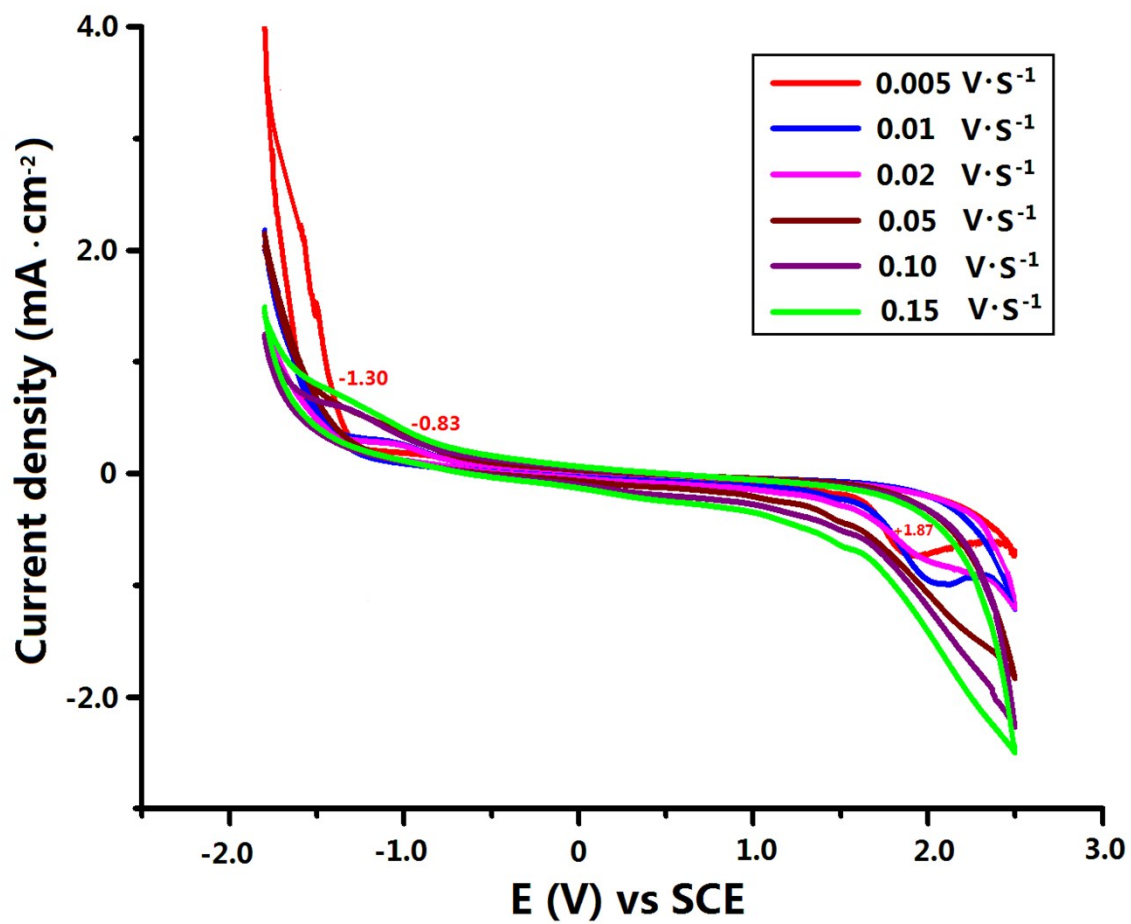


Fig. S7 CVs of 2-GCE in a 0.4 M acetic acid- sodium acetate buffer solution (pH = 4.5, 50 mL) in the potential range from -1.8 to 2.5 V vs SCE at different sweep rates.

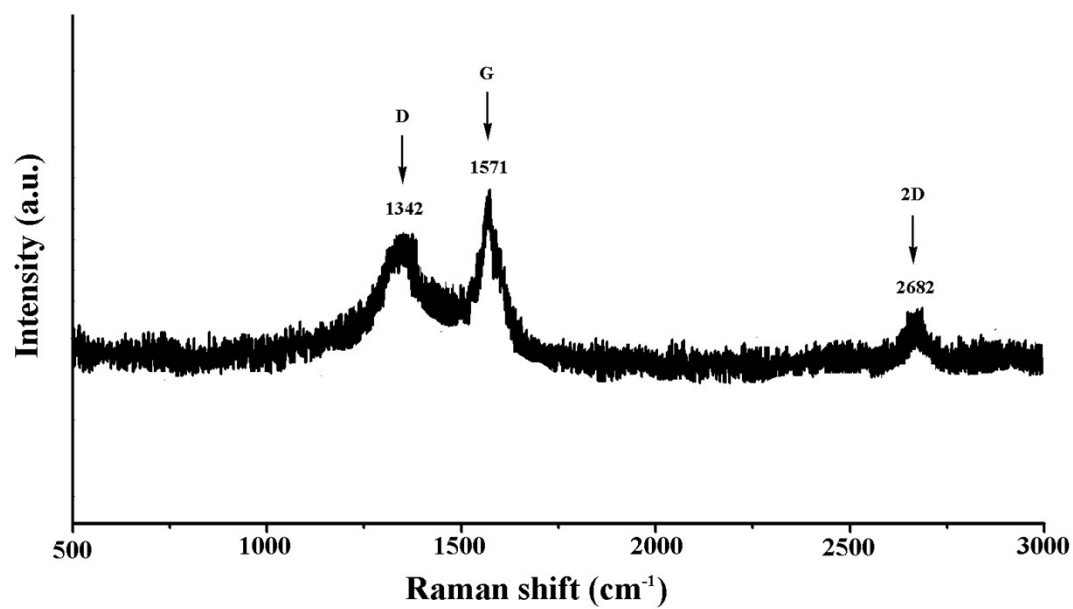
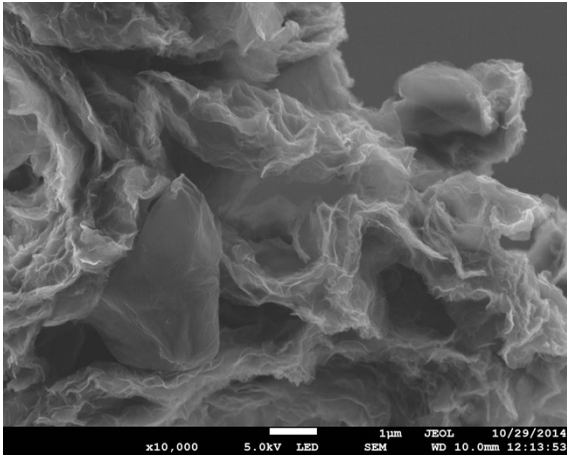
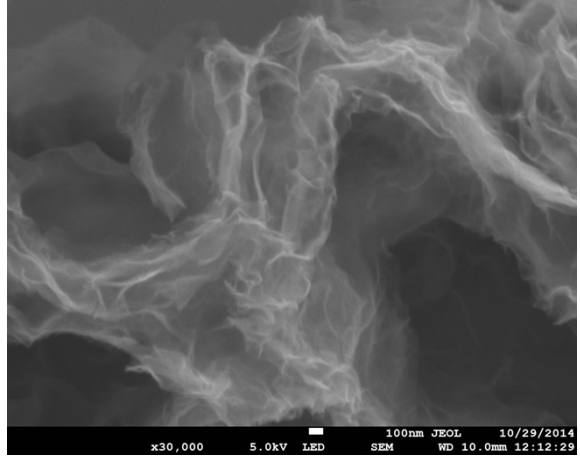


Fig. S8 Raman spectrum ($\lambda_{\text{ex}} = 514.5 \text{ nm}$, 0.4 mW) of the graphene.

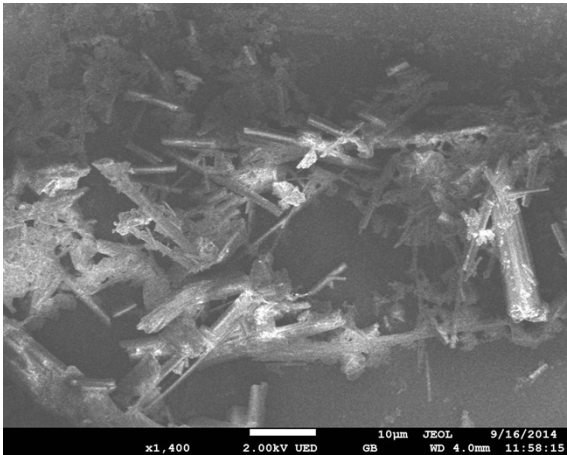
(a)



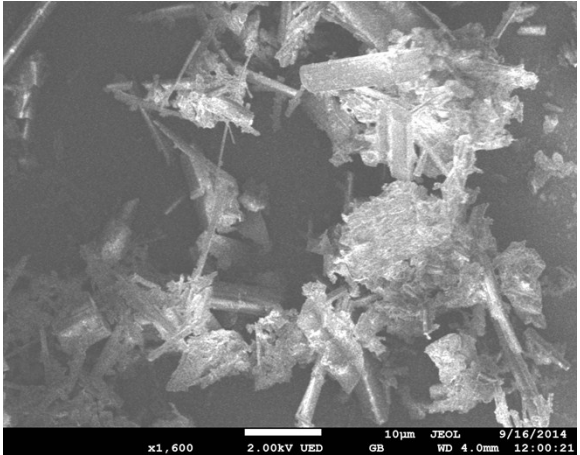
(b)



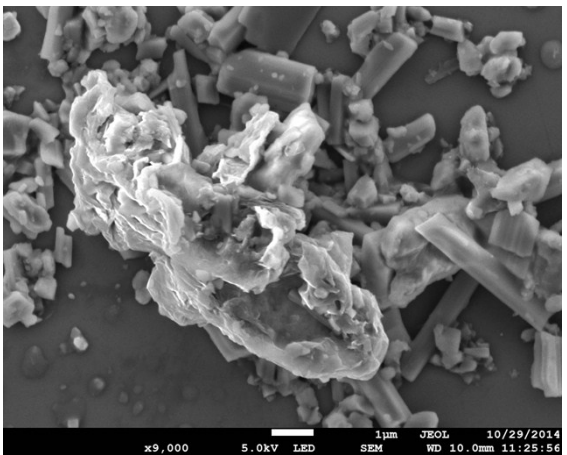
(c)



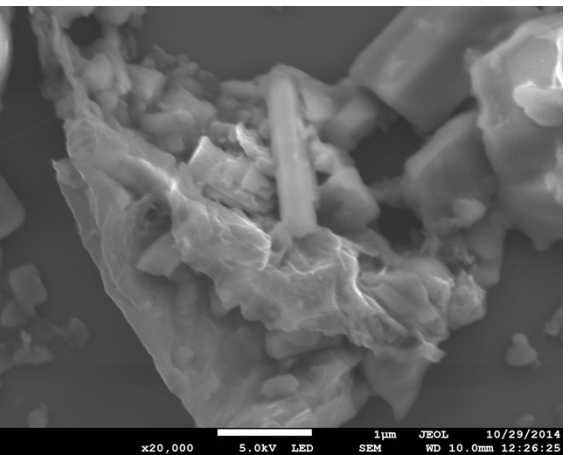
(d)



(e)

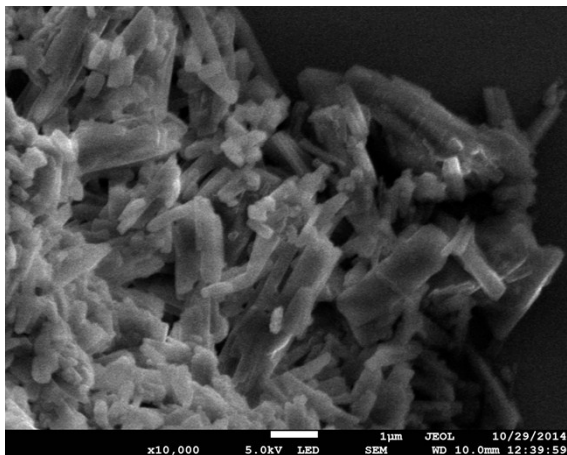


(f)

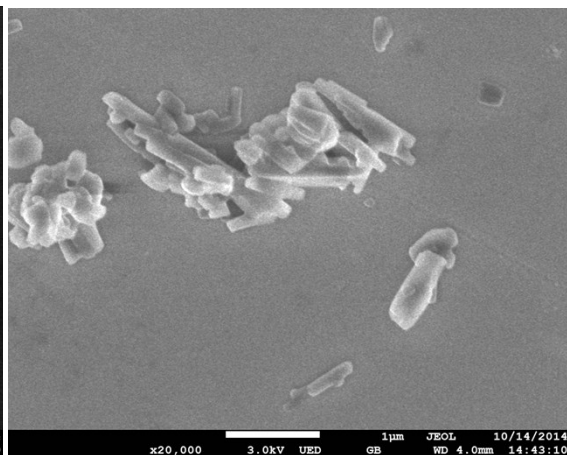


(g)

(h)



(i)



(j)

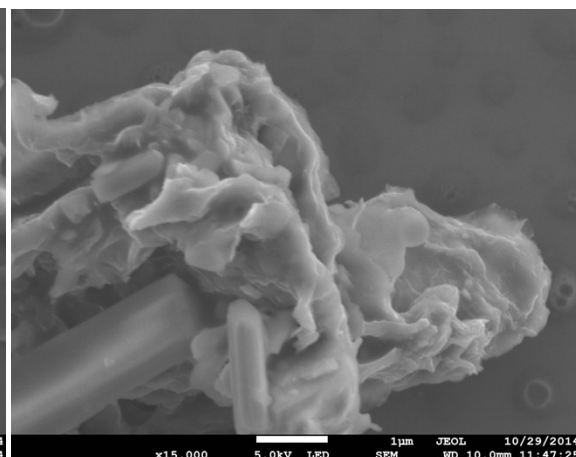
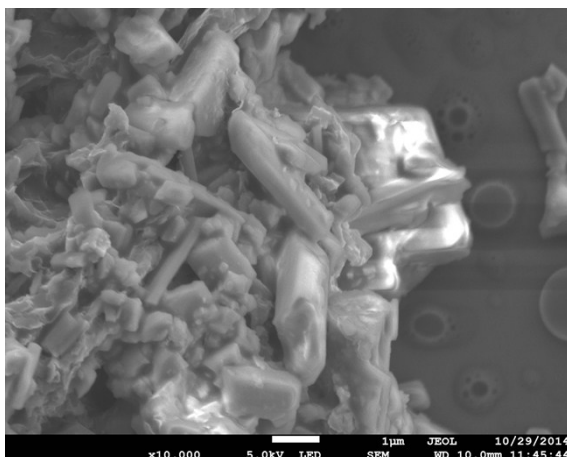


Fig. S9 The SEM images of the graphene (a, b), complex 1 (c, d), 1/graphene composite (e, f), complex 2 (g, h) and 2/graphene composite (i, j).

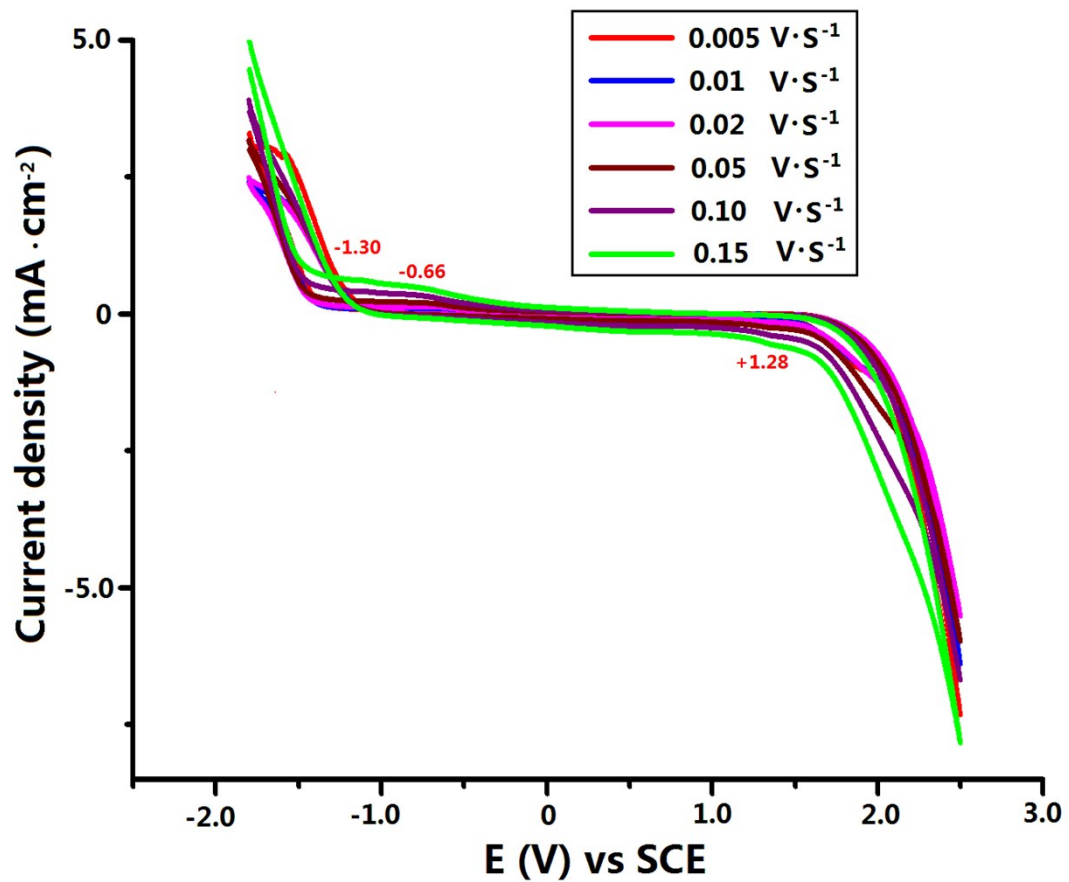


Fig. S10 CVs of 1/graphene-GCE in a 0.4 M acetic acid- sodium acetate buffer solution (pH = 4.5, 50 mL) in the potential range from -1.8 to 2.5 V vs SCE at different sweep rates.

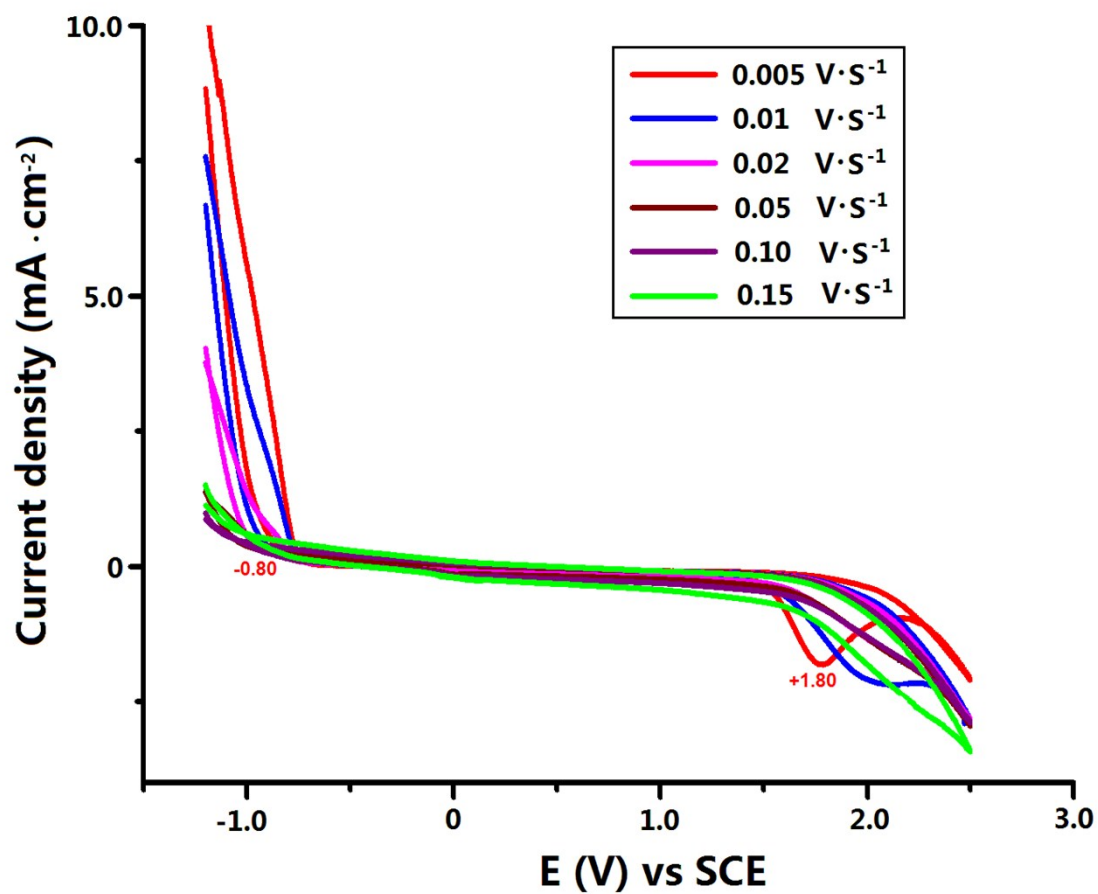


Fig. S11 CVs of 2/graphene-GCE in a 0.4 M acetic acid- sodium acetate buffer solution (pH = 4.5, 50 mL) in the potential range from -1.2 to 2.5 V vs SCE at different sweep rates.

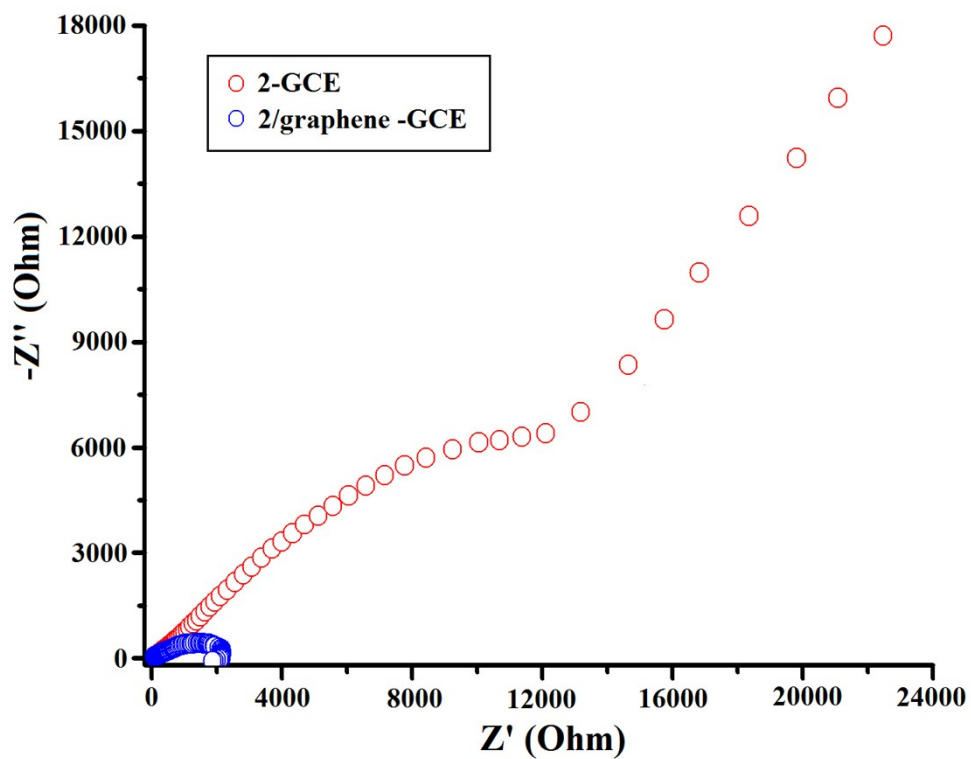


Fig. S12 Nyquist plots (Z' vs. $-Z''$) of the three-electrode systems in 0.4 M acetic acid-sodium acetate buffer solution (pH = 4.5, 50 mL) at the initial potential of -1.0 V vs SCE with 2-GCE and 2/graphene-GCE as working electrodes, respectively.

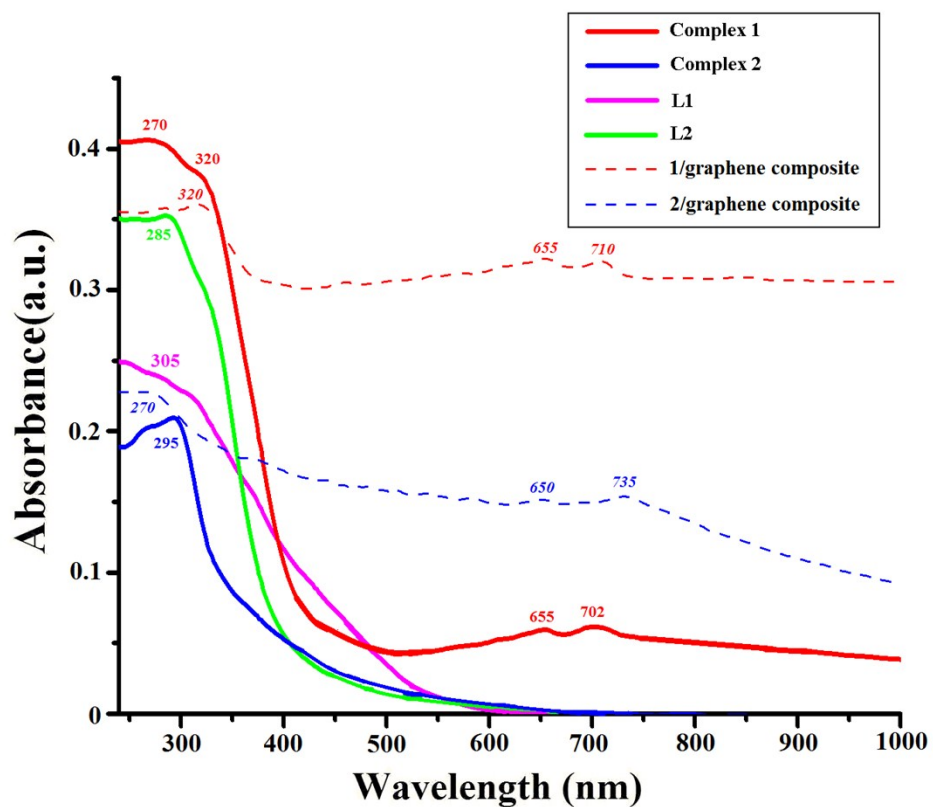


Fig. S13 UV-Vis absorption spectra at room temperature for the free ligands L1, L2, complexes 1-2 and their graphene composite materials.

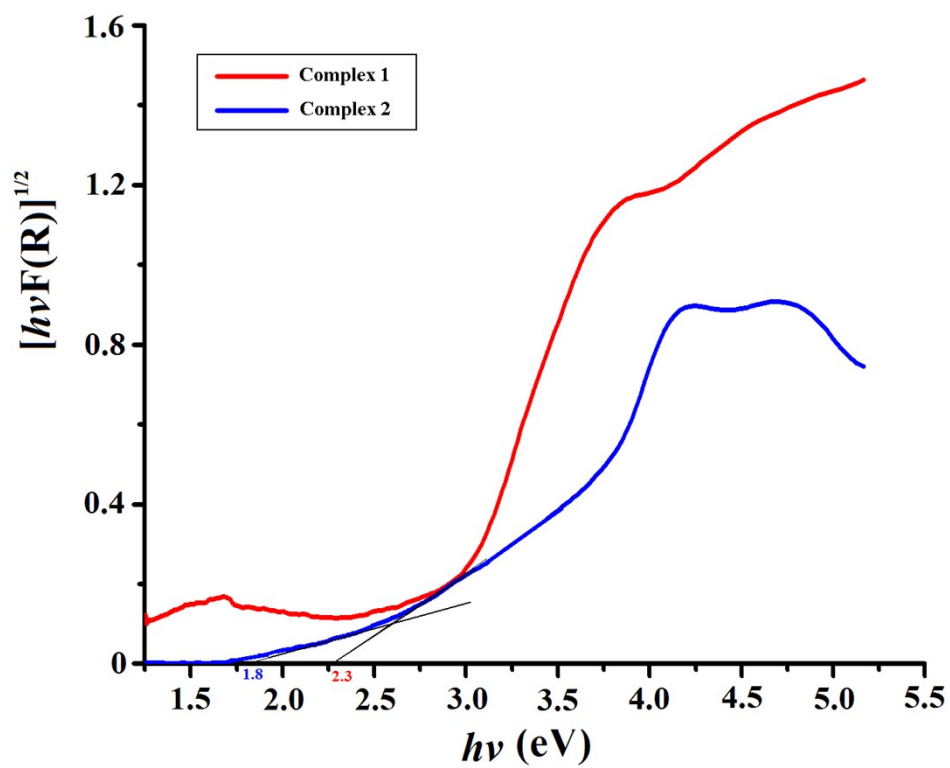


Fig. S14 The diffuse reflectance spectra for complexes **1** and **2** in Kubelka–Munk functions.

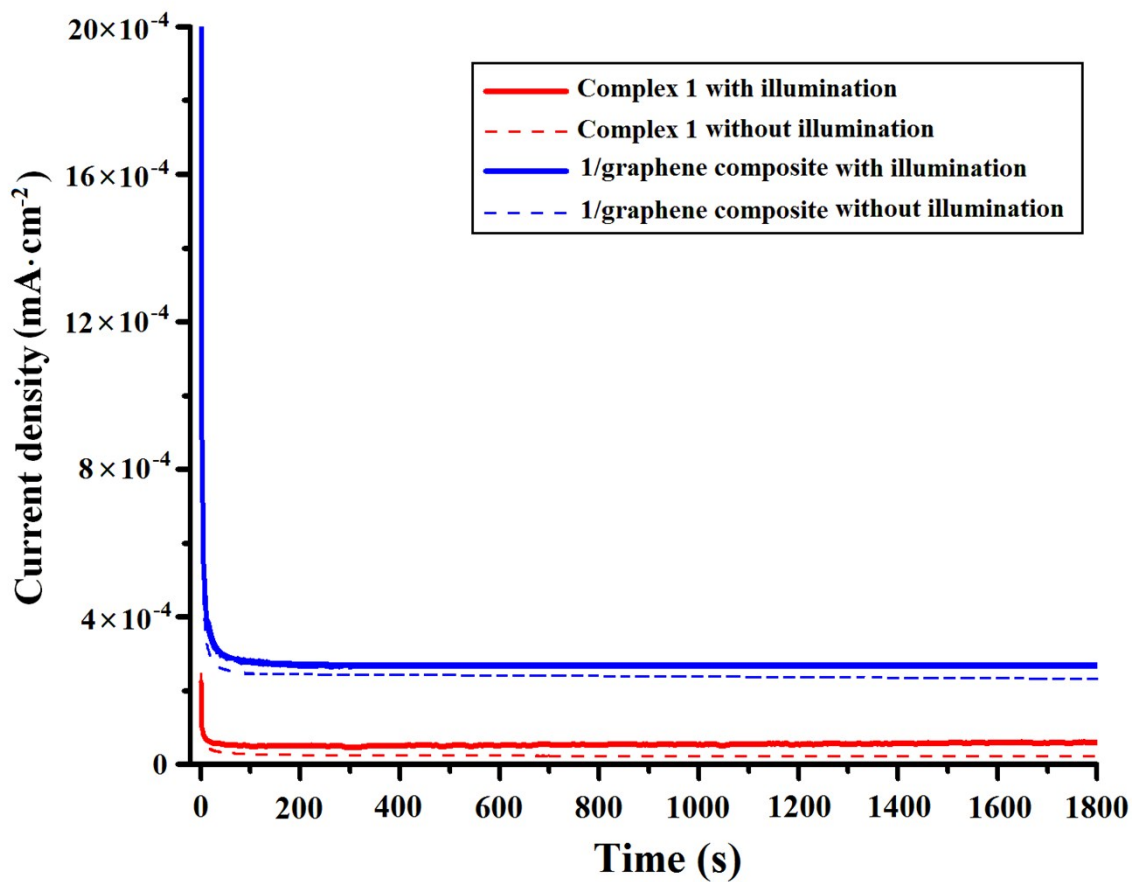


Fig. S15 Current-time curves for complex 1- and 1/graphene composite-modified FTO electrodes in the absence (dotted lines) and presence of visible light illumination (solid lines) ($650 \text{ nm} > \lambda > 350 \text{ nm}$) at $100 \text{ mW}\cdot\text{cm}^{-2}$ with the open circuit potential of 0V vs Ag/AgCl was applied to the electrodes.

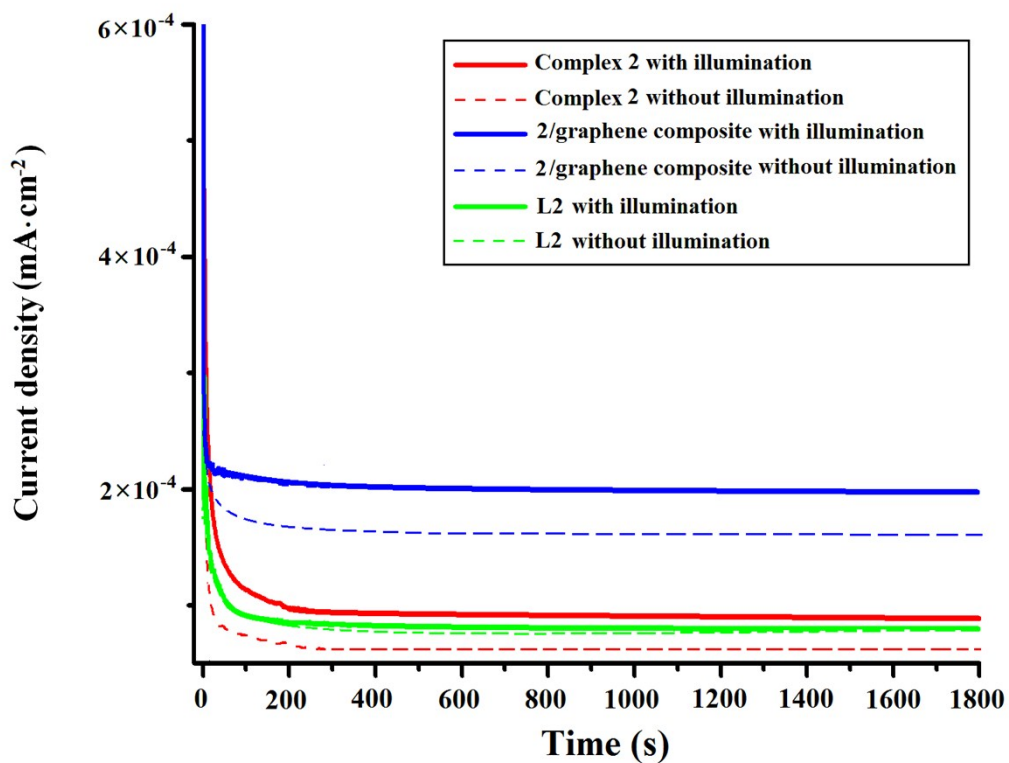


Fig. S16 Current-time curves for L2-, complex 2- and 2/grapheme composite-modified FTO electrodes in the absence (dotted lines) and presence of visible light illumination (solid lines) ($650 \text{ nm} > \lambda > 350 \text{ nm}$) at $110 \text{ mW}\cdot\text{cm}^{-2}$ with the open circuit potential of 0V vs Ag/AgCl was applied to the electrodes.

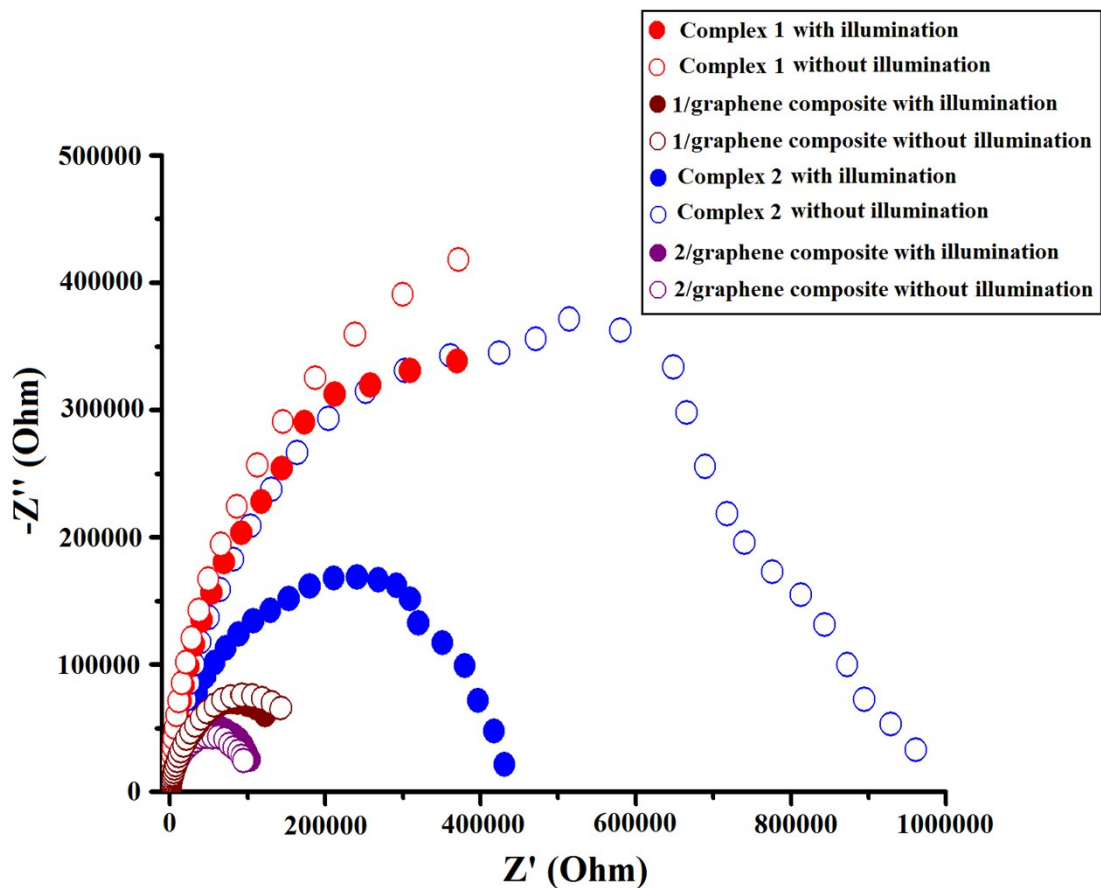


Fig. S17 Nyquist plots (Z' vs. $-Z''$) of the three-electrode systems at $E = 0$ V vs Ag/AgCl in acetic acid- sodium acetate buffer solution (0.4 M, pH = 4.5, 50 mL) in the absence and presence of visible light illumination ($650 \text{ nm} > \lambda > 350 \text{ nm}$) with the complexes- and their graphene composites-modified FTO slides as working electrodes, respectively.

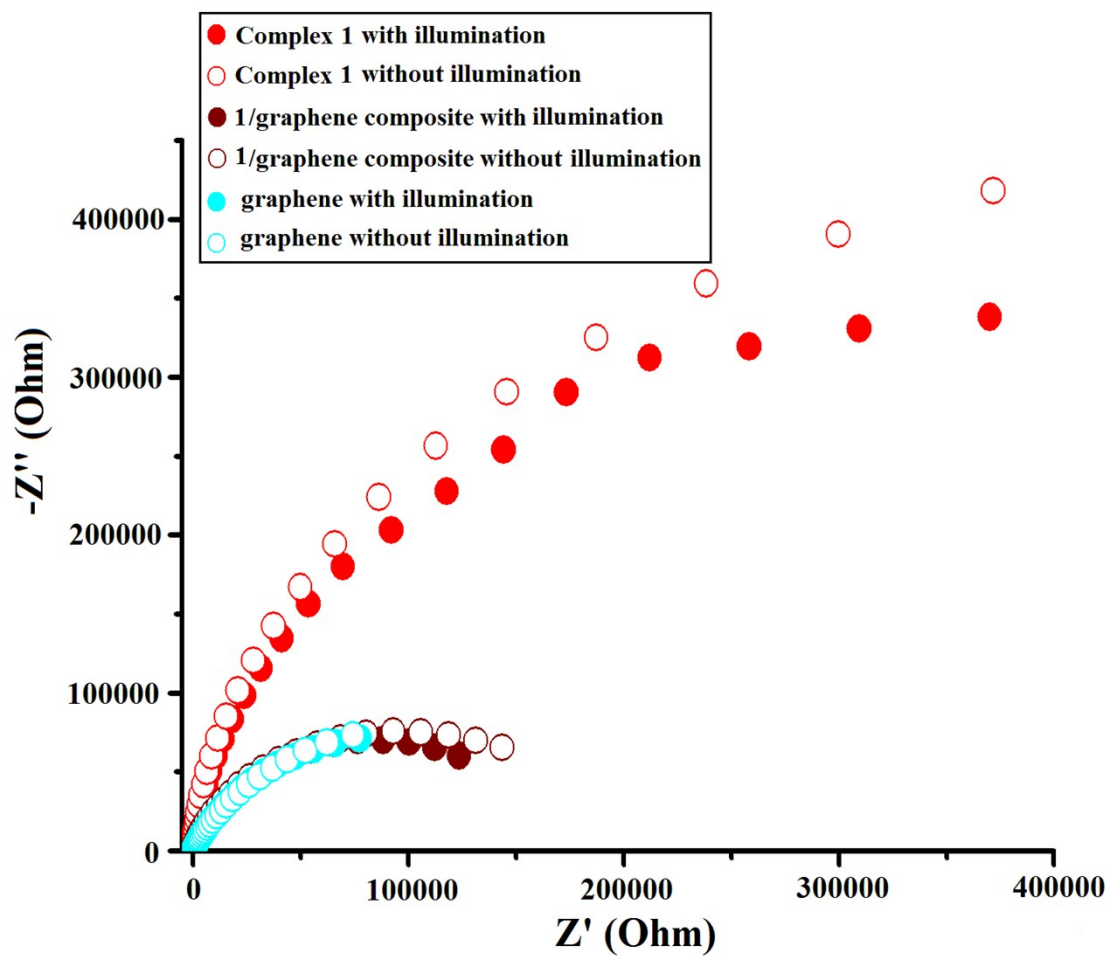


Fig. S18 Nyquist plots (Z' vs. $-Z''$) of the three-electrode systems at $E = 0$ V vs Ag/AgCl in acetic acid- sodium acetate buffer solution (0.4 M, pH = 4.5, 50 mL) in the absence and presence of visible light illumination ($650 \text{ nm} > \lambda > 350 \text{ nm}$) with graphene-, 1- and 1/graphene composite- modified FTO slides as working electrodes, respectively.

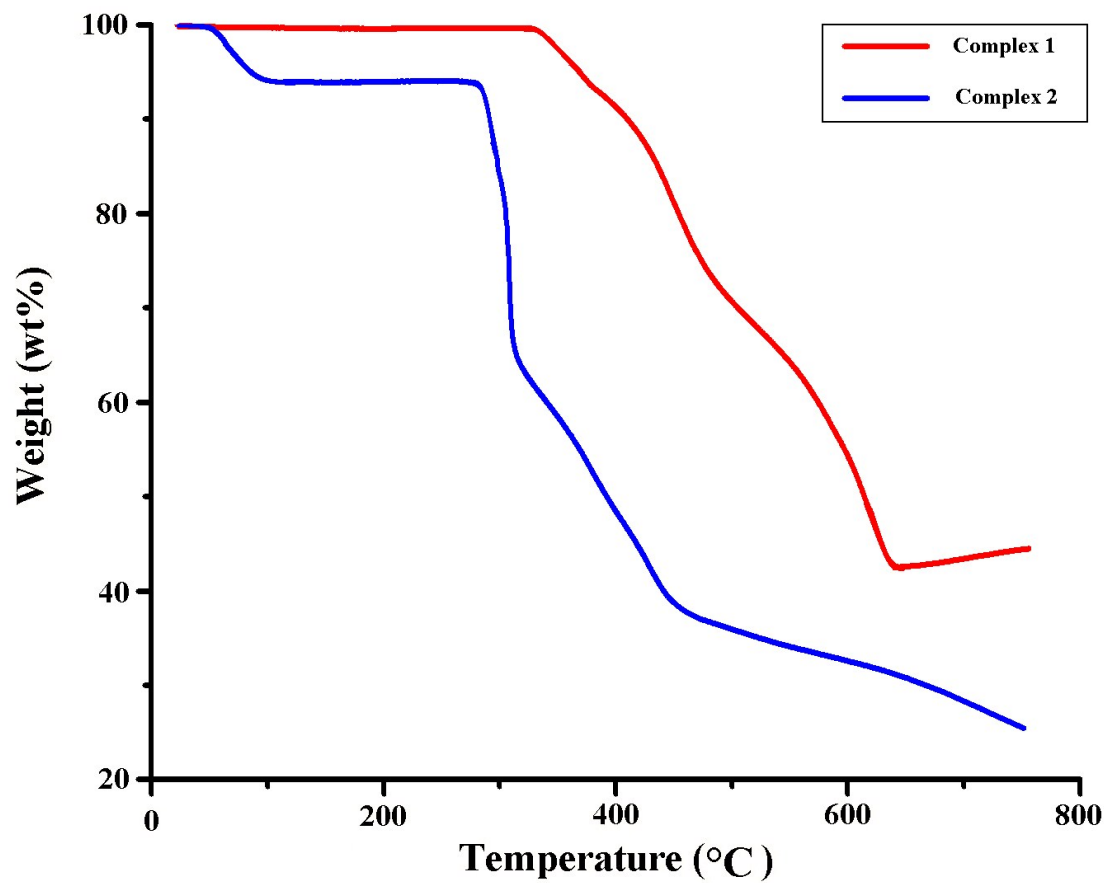


Fig. S19 Thermogravimetric curves of complexes 1 (red) and 2 (blue).